

The Implementation of AI Based Fracture Modeling to Conquer the Challenges in Unconventional Tight Limestone Reservoir

Kim Long Nguyen¹, Meshael Jumah¹

¹Kuwait Oil Company

Extended Abstract

Abstract

Carbonate reservoir usually presents a complex and heterogeneous distribution of fractures influenced by diverse factors, such as stress mechanism, seismic resolution, lithological properties, etc. The complexity poses challenges for high-resolution 3D modeling and characterization, which led to unsuccessful result of development wells since fracture intensity significantly impacts the reservoir connectivity and production sustainability. Therefore, Artificial Neural Networks (ANN) technology has been implemented to tackle these challenges due to its supremacy in data integrity to predict outcomes by assimilating multiple inputs without bias, using supervised or unsupervised machine learning methods. A comprehensive Continuous Fracture Modeling (CFM) workflow is established using ANN approach to analyze the relationship between 3D seismic attributes and fracture intensity logs derived from borehole image (BHI) data, enabling both qualitative and quantitative evaluation to increase the level of confidence in reservoir assessment. The aim is to generate 3D fracture intensity model, and efficiently identify fracture sweet spots to strategize field development plan including upcoming well placements.

Introduction

Kra Al-Marū (KM) field, locates in western Kuwait, was discovered in 1995 by the initial exploration Well-A ([Fig. 1](#)). Structurally, the field is characterized by a four-way closure trending NW-SE, and bounded by dominant NE- SW faults. Additionally, a regional East-West fault intersects the northern part of the KM field, which exhibits no visible displacement on seismic. Najmah (NJ) and Sargelu (SR) Formation are the main reservoirs in KM field, which deposited in Middle Jurassic. NJ Formation is represented by highly variable lithologies, hence a wide range of reservoirs & system trap is present.

The sediments comprise first the organic-rich limestone that represents deposition in an anoxic outer ramp to basin environment. They are contemporaneous with important Oceanic Anoxic Events (OAE). These OAE are associated with major flooding events of Jurassic time in many areas (G. Gega, 2017). The formation is subdivided into four units ([Fig. 2](#)): Upper NJ shale (NJW-1), Upper NJ limestone (NJW-2), NJ kerogen (NJW-3,-4,-5), Lower NJ limestone (NJW-6). NJ Kerogen is an organic-rich layer, and it plays a crucial role as a hydrocarbon kitchen for NJ- SR reservoirs. Lower NJ limestone, the amalgamated interval of organic-rich and limestone layers, is one of the key production contributors beside Sargelu reservoir which is clean limestone & fractured-driven. Being more fractured, Upper Sargelu (SRW-1) stands out as the best productive interval in Najmah-Sargelu.

Legacy exploration in KM field has confirmed the potential of hydrocarbon, but it posed challenges of production sustainability when wells failed to adequately penetrate fracture clusters and optimized reservoir contact. Well- F, the first development well in the field, has been drilled to target fracture corridor along pre-defined lineaments (Fig. 3) identified through seismic attribute analysis. However, the preliminary result showed poor potential that triggered the crucial requirement to re-evaluate the fracture sweet spots in the field. In principle, the idea is to deploy ANN technology to derive 3D fracture intensity model. Despite the longstanding awareness of naturally fractured reservoirs in the Oil & Gas industry, they remain challenging due to inherent uncertainties. Unlike clastic sandstone reservoirs, where spatial correlations within sedimentary layers can be straightforwardly assumed, understanding the distribution of fractures is hindered by significant heterogeneity at large scales. The ANN approach ensures the assessment of fracture distribution in multi-direction (lateral & vertical) as well as multi-evaluation (qualitative and quantitative). The study preceded the derivation of Well-F's testing result. Consequently, the well was not included in the ANN model but served as a blind test to verify operational effectiveness. The ANN model's validity was subsequently leveraged to refine and optimize the ongoing drilling strategy.

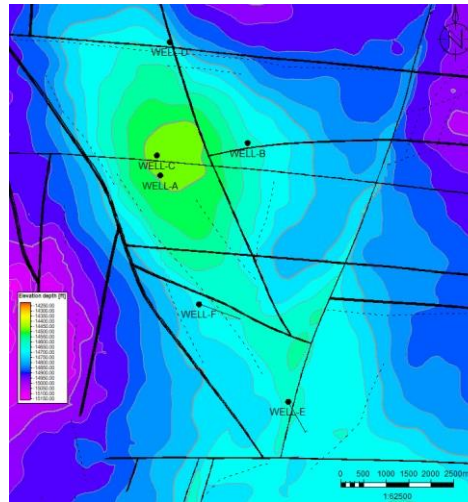


Fig. 3 Pre-defined lineaments (dotted line) in KM field

Methodology

The purpose of ANN was to autonomously establish relationships between multiple known variables and a single unknown variable. Specifically, there were known parameters, such as natural fractures identified by BHI or seismic attributes. Meanwhile, the unknown parameter was fracture intensity at the planned well. The proposed workflow (Fig. 4) consisted of fracture drivers derived from seismic attribute analysis that might require a large variety of attributes including Ant Tracking, Local Flatness, Variance, Chaos, Curvatures, Dip, Azimuth, etc.

In parallel, natural fractures were interpreted from BHI data, and they were used to integrate with seismic attribute maps by using ANN models. Each individual element was computed and connected in the neural networks. The connection was managed by weights, which was the influence of each element in the ANN models. ANN came in two primary types: unsupervised and supervised. In this study, the supervised ANN was utilized, requiring input-output pairs of training data provided by the user. Through the Train Estimation Model process, these data pairs were used to create a model of fracture intensity in three dimensions.

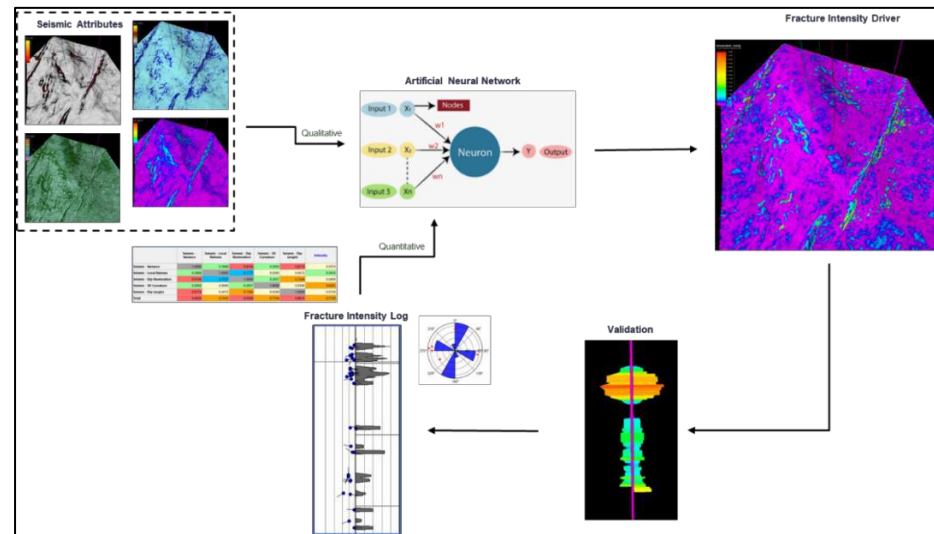


Fig. 4 Artificial Neural Network (ANN) Workflow

Initially, natural fractures were identified using BHI data from key wells (Well-B, Well-C, Well-D, and Well-E). Individual fractures were interpreted from these logs and analyzed by plotting their poles in the upper hemisphere using equal-area projection to assess the overall pattern and identify potential fracture sets. The dominant strike orientation of all fractures was clearly determined (Fig. 5). It was apparent that dominant fractures in the KM field following NNE-SSW to NE-SW direction, which aligned regional tectonic setting.

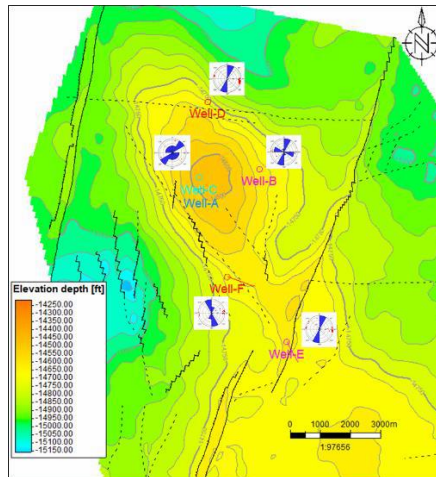


Fig. 5 Dominant strike of fractures in SRW-1 reservoir

The fracture intensity log for each key well was generated by moving a triangular window along the borehole, creating a virtual log that correlated with observed fractures and quantified their density per unit length (Fig. 6). Three versions of the fracture intensity log were produced using different window lengths: 5ft, 10ft, and 20ft. After evaluation, a 10ft window was selected as it struck a balance between preserving detailed data and smoothing out noise, thus defining the BHI fracture intensity log. Among the exploratory wells, Well-D notably exhibited the highest fracture count, situated in the shattered zone in the northern part of the KM field where a significant E-W seismic lineament cut across the area (Srigiriraju et al., 2012). Following closely was Well-E, intersecting a major NE-SW fault and consequently displaying a high fracture intensity. Conversely, Well-F showed the lowest fracture density, intersecting a sub-seismic zone with minimal fracture occurrence. As previously mentioned, Well-F was designated for a blind test and therefore excluded from the ANN analysis.

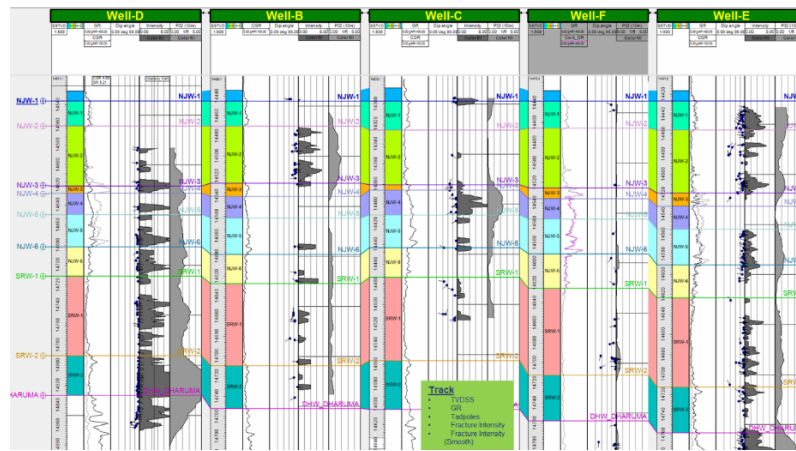


Fig. 6 Fracture Intensity Log generated from Borehole Image log interpretation

To establish a fracture intensity model, the ANN integrated volumetric data such as seismic attributes or geomechanical properties cubes. Hence, a range of seismic attributes was scrutinized, including Curvature, Ant Tracking, Variance, Chaos, and Local Flatness, among others. These attributes were scaled up for modeling and cross-referenced with fracture intensity data obtained from wells, undergoing both qualitative and quantitative analyses. Qualitatively, seismic attributes demonstrated a strong correspondence with fracture indicators from wells (Fig. 7). Notably, Well-D and Well-E were situated in favorable fracture sweet spots, contrasting with others exhibiting fewer fractures. This observation correlated well with drilling and testing outcomes. Quantitative analysis involved calculating correlation coefficients between each seismic attribute and the fracture intensity log, ranking them accordingly. Attributes showing coefficients closer to 1 indicated a stronger correlation. Notably, Curvature emerged as the most influential attribute for input into the ANN model, boasting the highest correlation coefficient (0.63) with the BHI fracture intensity log among the attributes assessed. Overall, while correlation coefficients generally did not reach high levels, emphasizing the necessity of employing Artificial Neural Networks to address the complexities.

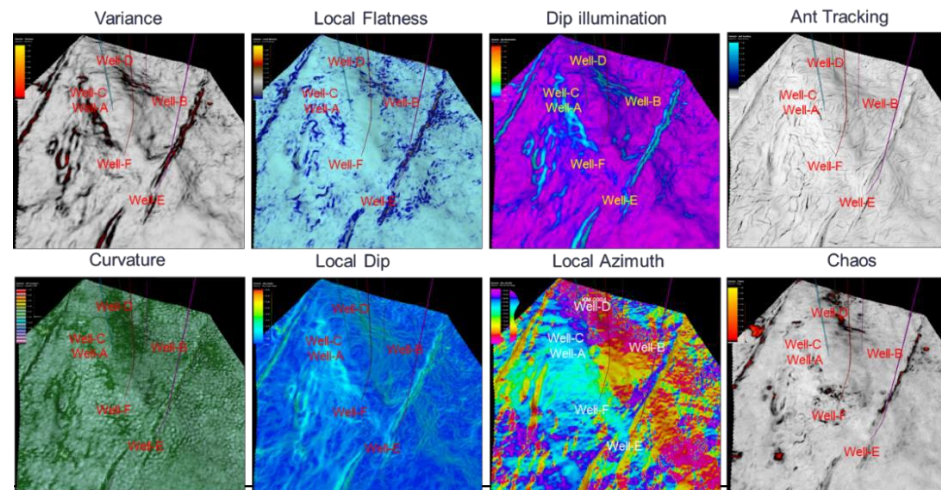


Fig. 7 Seismic attribute analysis in KM field at SRW-1 reservoir

Following rigorous evaluation based on both qualitative and quantitative criteria, five seismic attributes including Variance, Local Flatness, Dip Illumination, 3D Curvature, and Dip Angle were selected for inclusion in the ANN modeling process (Fig. 8).

	Seismic - Variance	Seismic - Local flatness	Seismic - Dip illumination	Seismic - 3D Curvature	Seismic - Dip (angle)	Intensity
Seismic - Variance	1.0000	0.3888	0.9194	0.3950	0.8174	0.5574
Seismic - Local flatness	0.3888	1.0000	0.1727	0.5095	0.4572	0.3419
Seismic - Dip illumination	0.9194	0.1727	1.0000	0.3937	0.7264	0.5409
Seismic - 3D Curvature	0.3950	0.5095	0.3937	1.0000	0.5599	0.6291
Seismic - Dip (angle)	0.8174	0.4572	0.7264	0.5599	1.0000	0.5729
Total	0.9639	0.7452	0.9509	0.7104	0.8615	0.7156

Fig. 8 Quantitative analysis of seismic attributes vs Borehole Image fracture intensity log

All aforementioned seismic attributes were input to Artificial Neural Network Model with supervised mode. The BHI fracture intensity log was used as supervised data to control the propagation of fracture intensity model:

- Maximum number of iterations: 100. When this amount of iteration was done, the process will stop whether or not the error limit had been reached.
- Error limit: 15. When the remaining error reached this point, the iterations will stop.
- Cross validation: 70. The percentage of supervised data that was used in cross validation.

Consequently, the output from the ANN was a 3D model (Fig. 9) depicting fracture intensity across both horizontal and vertical axes. The model highlighted consistent high-faulted zones, particularly along preserved NE-SW faults, as evident in Well-E, which penetrated a faulted zone. The western flank of the KM field near Well-A and Well-C exhibited prominent high-intensity features running NW-SE. Additionally, the fracture intensity model reflected E- W faults in the southern area near Well-D. In the crestal area where Well-A, Well-B, and Well-C are located, the model illustrated lower fracture intensity. This raised questions regarding the promising testing results obtained from these wells despite lacking high fracture sweet spots. It was speculated that the fractures encountered in these wells were conjugate fractures because of folding process on highest anticlinal crest of the field. Meanwhile, the fractures along the faults were classified as fracture corridors.

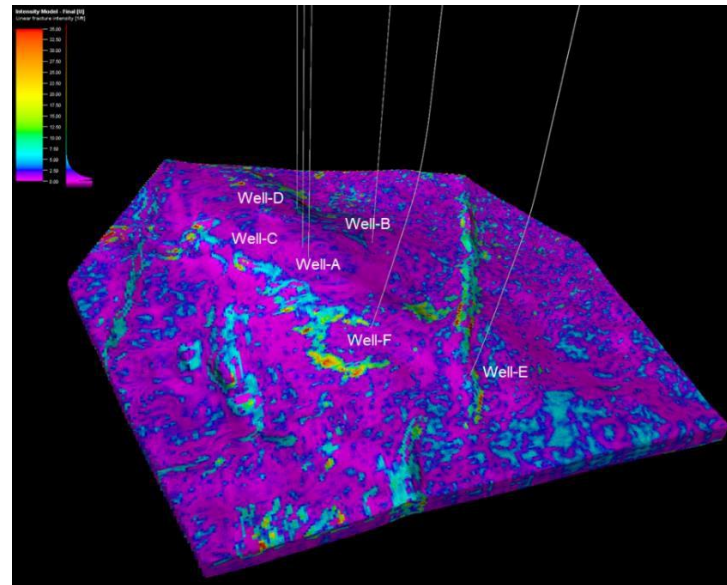


Fig. 9 3D Fracture intensity model (SRW-1 reservoir)

To ensure quality control of the output, pseudo log was generated from the model and compared against the BHI fracture intensity log from exploratory wells (Fig. 10). The comparison revealed a highly accurate alignment between these variables. Further validation through a cross-plot analysis (Fig. 11) confirmed a strong relationship with a correlation coefficient of 0.91. To achieve a precise alignment with the BHI log at each exploratory well, the ANN model was utilized as a co-kriging variable to guide the propagation of BHI fracture intensity logs.

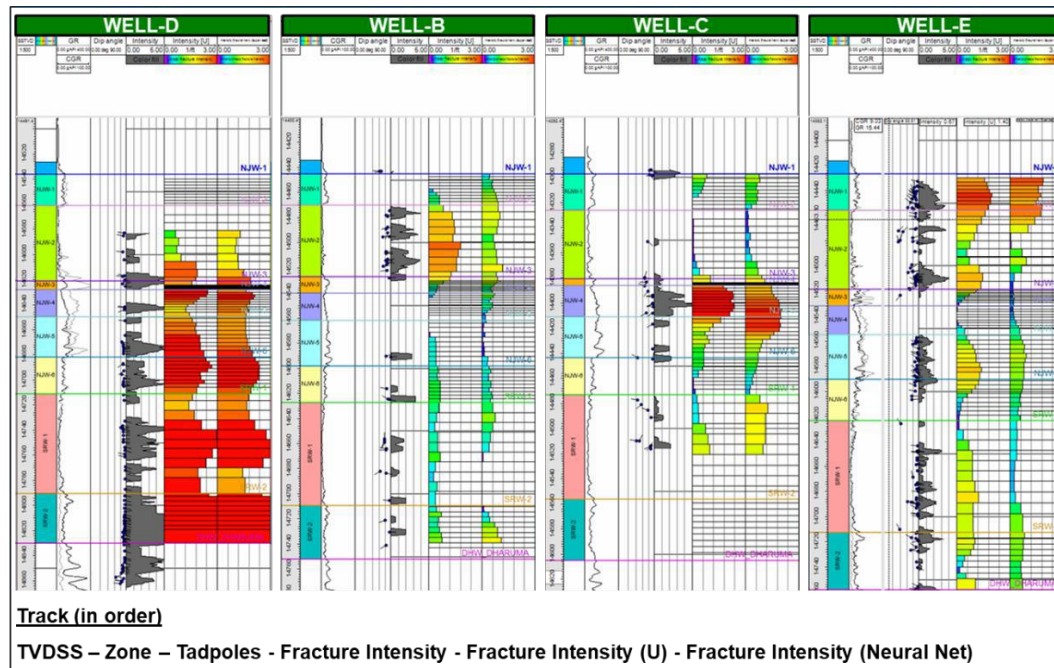


Fig. 10 Comparison between ANN derived vs BHI fracture intensity log

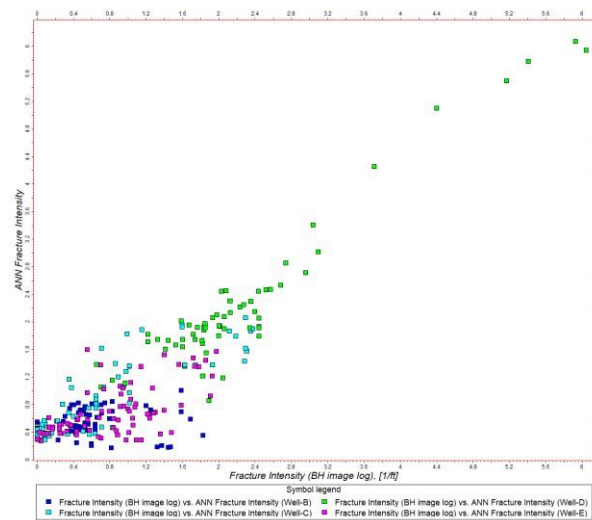


Fig. 11 Cross-plot of ANN derived vs BHI fracture intensity log. Correlation Coefficient (R2) is 0.91

In order to validate the ANN model by blind test, a pseudo log of fracture intensity was generated in Well-F and compared with BHI fracture intensity log. If the result was not matching then the ANN model was rerun with variation of input parameters in order to derive a desirable output. According to prior assessments, Well-F was anticipated to intersect the NW-SE lineament and associated fractures. However, well data revealed an unexpected encounter with a low fracture intensity zone (Fig. 12). This observation aligned with the average fracture intensity map generated using ANN methodology (Fig. 13).

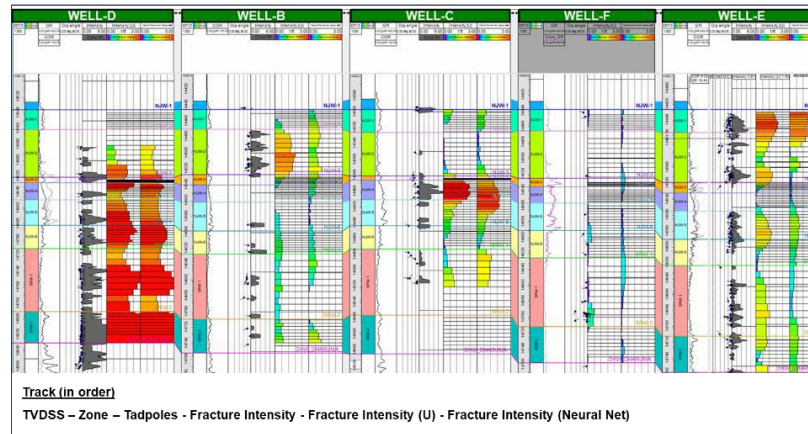


Fig. 12 Validation of ANN model from blind test on Well-F

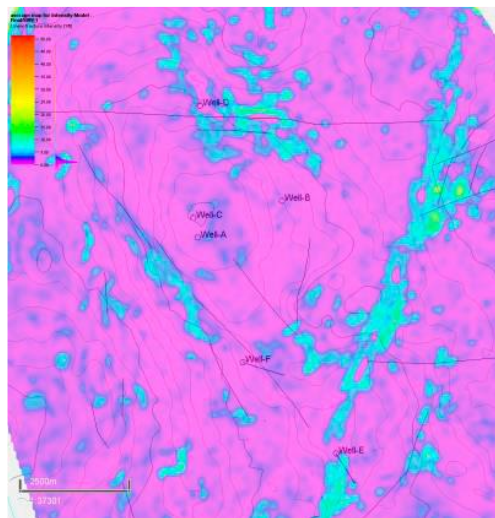


Fig. 13 Average map of fracture intensity model in SRW-1 reservoir

Consequently, the flow test of Well-F revealed significantly poor performance. Based on this validation, it was concluded that the well failed to intersect fractures along the NW-SE lineament. This outcome necessitated the re-evaluation of the lineaments within the KM field, particularly in the central area adjacent to Well-B and Well-F

The ANN model result identified two new fracture sweet spot areas (Fig. 14.a) within the crestal part of the field, in addition to the existing NNE-SSW trending zone on the eastern down-flank:

- South of Well-D
- Southwest of Well-A

The eastern flank of the KM field also showed high fracture sweet spots developing along the NE-SW major fault. However, these areas were disregarded due to their distance from the structure, posing a higher risk of fluid contact. The findings of the ANN fracture intensity model were consistent with observations from flow performance in exploratory wells. With high confidence in the ANN findings, two new wells (Well-G & Well-H) were proposed (Fig. 14.b) to drill in these defined sweet spots to enhance reservoir connectivity (high fracture intensity) and maximize reservoir contact (utilizing a high-deviated well profile aligned with NW-SE drilling direction).

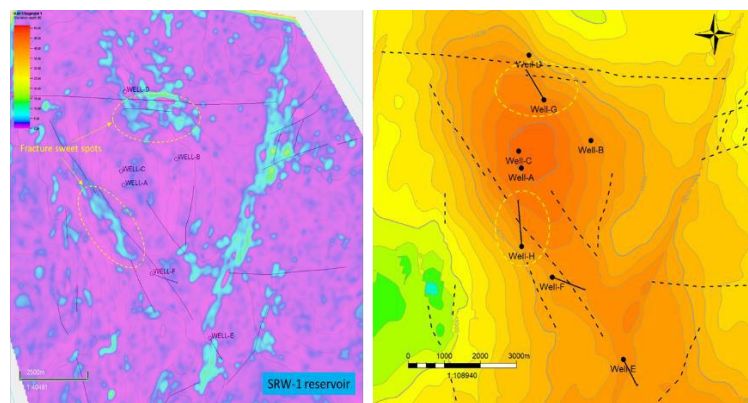


Fig. 14 Sweet spot areas identified from fracture intensity model (a) & Proposed development wells (b)

Result & Discussion

Well-G was designed as highly deviated profile to maximize the intersection of natural fractures. The result clearly demonstrated that the well has entered fracture sweet spots reflected in mudlogging data with series of gains/losses in NJW-6 & SRW-1 reservoir (Fig. 15) which led to concerns on well control & cancelling of logging acquisition. This resulted the unavailability of BHI data to ascertain the presence of natural fractures. Despite of uncertainties, the well was tested that resulting excellent outcome with high flow rate of light oil, high reservoir pressure, and without water cut.

Fig. 16 Excellent match in fracture detections among three methods of Borehole Image, Deep Shear Wave Imaging, and Coriolis Flowmeter in SRW-1 reservoir (red box)

Conclusion

Fracture prediction plays a crucial role in evaluating and developing fracture reservoirs. However, accurately characterizing fractures is challenging due to their extreme heterogeneity stemming from complex genetic factors. Furthermore, technological limitations persist in effectively addressing these challenges. In this study, Artificial Neural Networks were proposed as a viable solution for fracture modeling and characterization, leveraging their superior capabilities in data prediction and estimation. The ANN approach successfully identified high fracture intensity sweet spots within the KM field. Results demonstrated a strong correlation between the fracture intensity model generated by ANN and the fracture intensity log from the BHI tool. This alignment was further validated by consistent production performance observed in exploratory wells across the KM field. Moreover, ANN modeling provided insights into specific scenarios, such as explaining the low fracture intersection observed in Well-F, the initial development well. It also delineated potential areas of high fracture intensity within the field resulting the placement of two development wells (Well-G & Well-H).

The productive outcomes of Well-G & Well-H have confirmed the validity of ANN method applied to tackle the technical challenges in NJ-SR fractured tight limestone reservoir. This innovative workflow significantly refined the development strategy by enhancing production potential and reducing drilling and testing costs for the company. The demonstrated efficacy of ANN methodology underscores its relevance and applicability for fracture characterization, not only in the KM field but also across other areas in West Kuwait.

Acknowledgement

The authors would like to express special thanks to Kuwait Oil Company & Ministry of Oil for granting permission to publish the paper.

Abbreviations

<i>ANN</i>	<i>Artificial Neural Network</i>
<i>BHI</i>	<i>Borehole Image</i>
<i>CFM</i>	<i>Continuous Fracture Modeling</i>
<i>DSWI</i>	<i>Deep Shear Wave Imaging</i>
<i>KM</i>	<i>Kra Al-Marū</i>
<i>NJ-SR</i>	<i>Najmah-Sargelu</i>
<i>WK</i>	<i>West Kuwait</i>

References

A.K.E Ouahed et al. 2005. Application of Artificial Intelligence to Characterize Naturally Fractured Reservoirs Journal of petroleum Science and Engineering, Vol 49, Issues 3-4. 15th December, Pages 122-141. <https://doi.org/10.1016/j.petrol.2005.05.003>

- D. Hasanusi et al. 2012 . Fracture and Carbonate Reservoir Characterization using Sequential Hybrid Seismic Rock Physics, Statistic and Artificial Neural Network: Case Study of North Tiaka Field. Presented at GEO Manama, Bahrain, 4th March. cp-287-00108.
<https://doi.org/10.3997/2214-4609-pdb.287.1180851>
- G. Gega, et al. 2017. The Stratigraphic Traps of Najmah Formation in Kuwait. Presented at AAPG/Middle East GTW, Stratigraphic Traps of the Middle East, December 11-13, 2017, Muscat, Oman.
- G. Sabinin et al. 2020. Machine Learning for Fracture Parameter Estimation in Fractured Reservoirs from Seismic Data. Paper presented at the SPE Russian Petroleum Technology Conference, Virtual, 26th October. Paper Number SPE-201934-MS. <https://doi.org/10.2118/201934-MS>
- M. Adibifard, S.A.R Tabatabaei-Nejad, and E. Khodapanah, 2014. Artificial Neural Network (ANN) to estimate reservoir parameters in naturally fractured reservoirs using well test data. Published on Journal of Petroleum Science and Engineering, 22nd August.
<https://doi.org/10.1016/j.petrol.2014.08.007>
- Nguyen, et al. 2024. Ascertain the Presence of Open Fractures in Tight Carbonate Reservoirs with Integrated Solution. Presented at URTEC, Jun 17-19, 2024, Houston, TX, USA. <https://doi.org/10.15530/urtec-2024-4023323>
- Nguyen, et al. 2023. Identifying Fracture Sweet Spots Using Artificial Neural Network Approach: A Case Study in Najmah/Sargelu Reservoir, Kra Al-Marzuq Field, West Kuwait. Presented at Middle East Oil, Gas and Geosciences Show (MEOS) 2024, Manama, Bahrain.
<https://doi.org/10.2118/213770-MS>
- Nguyen, et al. 2024. Application of Gas While Drilling in Fluid Detection and Perforation Strategy in Jurassic Reservoirs. Presented at International Petroleum Technology Conference, February 2024. Dhahran, Saudi Arabia.
- O. Fonta, H.A.Ajmi, N.K. Verma, et al. 2007. The Fracture Characterization and Fracture Modeling of a Tight Carbonate Reservoir – The Najmah-Sargelu of West Kuwait. SPE Res Eval & Eng 10 (06):695-710. Paper Number: SPE-93557-PA. <https://doi.org/10.2118/93557-PA>
- O. Pinous, A.M. Zellou, G. Robinson, et al. 2007. Continuous Fracture Modeling of a Carbonate Reservoir in West Siberia. Presented at the International Oil Conference and Exhibition in Mexico held in Veracruz, Mexico, 27-30th June. SPE-103284-MS.
<https://doi.org/10.2118/103284-MS>
- O. Richard, S. Lamine, C. Pattnaik, et al. 2017. Integrated Fracture Characterization and Modeling in North Kuwait Carbonate Reservoirs. Presented at the Abu Dhabi International Petroleum Exhibition & Conference, Abu Dhabi, UAE, 13th November. SPE-188185-MS.
<https://doi.org/10.2118/188185-MS>

R.A Azim, T. Shehab, 2017. Estimation of Reservoir Fracture Network Properties Using an Artificial Intelligence Technique. Published on Journal of Applied Engineering Research, ISSN 0973-4562, Volume 12, Number 15 (2017) pp 5345-5350. <https://doi.org/10.30632/PJV61N3-2020a5>